HOLOS
ISSN 1807 - 1600

# PERFILAGEM ELÉTRICA DE DESAGUAMENTO DE AREIA INDUZIDO POR VIBRAÇÃO

**J. L. M. REIS [1], J. A. M. DA LUZ [2], F. VARDANEGA[3]**
Departamento de Engenharia de Minas, Universidade Federal de Ouro Preto[1,2,3]
ORCID ID: http://orcid.org/0000-0001-5390-5741 [1]
jonathanleandro39@yahoo.com.br

Submetido 30/08/2019 - Aceito 01/11/2020
DOI: 10.15628/holos.2021.8952

## RESUMO
A perfilagem eletrorresistiva da umidade no leito de areia quartzosa sobre tela vibratória em escala piloto foi tratado aqui. No que tange à configuração do eletrodos para medição de eletrorresistividade, o arranjo Wenner alfa clássico foi usado, exigindo espaçamento igual entre os eletrodos e mesma profundidade de penetração e alinhamento corretos. Aqui, a influência de pequenas variações na profundidade de penetração e falta de colinearidade dos eletrodos nas leituras de umidade, usando um eletrorresistivímetro digital e eletrodos de cobre, foi avaliada. As profundidades de penetração estudadas foram de 50 mm e 55 mm. Por sua vez, o desalinhamento testado dos eletrodos foi de 10 mm. O único fator que causou efeito estatisticamente significativo nas medições foi a profundidade de penetração de eletrodo, ao menos na faixa aqui estudada.

**PALAVRAS-CHAVE:** Desaguamento; Eletrorresistividade; Umidade, Arranjo Wenner alfa; Análise de sensibilidade.

# ELECTRICAL PROFILING OF VIBRATION-INDUCED DEWATERING OF SAND

## ABSTRACT
Electrorresistive profiling of moisture inside a quartz sand bed on a pilot-scale vibrating screen was treated here. As electrode or probe configuration for resistivity measurement is concerned, the classical Wenner α array was used, requiring equal electrode spacing, and correct penetration depth and alignment. Here, the influence of small variations in penetration depth and lack of probe collinearity on the moisture readings, using a digital earth resistance tester and copper wires as probes, was evaluated. The penetration depths studied were 50 mm and 55 mm. In turn, the electrode misalignment tested was 10 mm. The only factor that has caused statistically significant effect in measurements was probe penetration depth, at least under the range tested here.

**KEYWORDS:** Dewatering; Electroresistivity; Moisture; Wenner alpha array; Sensitivity analysis.

# 1 INTRODUCTION

Moisture of densified granular system is relevant in many instances the industry. The applicability of electroresistive profiling to quantify the variation of moisture inside quartz sand over a pilot scale vibrating screen, as a pre-drying operation, was treated in this paper. The electroresistivity method is usual in geophysical surveying, as exemplified by and Pandey et al. (2015), as well in other applications as in monitoring water content in concrete research (Bui et al., 2016). It encompasses the resistivity measurement of bulk material as function of porosity and other variables. Also recently, Ding and Chandra(2018) have used electroresistance (in consortium with Wi-Fi networks), in order to control soil moisture in plantations. As pointed out by Roodposhti et al. (2019) electrical resistivity method is a fast, non-invasive, and inexpensive method in geotechnical parameter prediction, such as soil moisture and compaction state of media.

The Wenner α probe array is applied to a number of studies involving electrical resistivity of granular or porous media. Although classically used for geophysical prospecting, it can be raised some examples of its application in other context, like one by Morris, Moreno and Sagüés (1996), that have employed this array for calibrating concrete probes porosity. In turn, Dahlin and Loke(1998) have used this kind of array for 2D imaging of geological features with aid of mathematical modeling.

Olayinka and Yaramanci (2000) have acquired geological data by Wenner $\alpha$ array and have gotten good results after inversion. Bristow *et alii* (2001) have conducted measurements of temperature, soil thermal diffusion, thermal capacity and conductivity, soil moisture and electrical conductivity. All these parameters have been obtained simultaneously via multielectrode arrangement in Wenner configuration and presented plausible responses.

Valente *et alii* (2006) have studied the data acquisition in silty soil zone, by Wenner arrangement, where the surveys were getting temperature, thermal properties, electrical conductivity, water flow rate and soil moisture. The results showed excellent statistical correlation.

Neyamadpour, Wan Abdullah and Taib (2010) have used the arrangement Wenner α, among others, for 3D imaging of lithological features. This technique proved to be the best among the surveyed ones.

In the study by Glover (2010) geophysical investigations were conducted comparing the arrangement of Wenner with that one of twin-probe. The Wenner excelled in better spatial resolution and detection of anomalies. Jolly, Beaven and Barker (2011) have applied the Wenner array in fluid seepage monitoring, obtaining satisfactory results, and, in some cases, superior over the conventional monitoring techniques. In the research conducted by Thabit and Khalid (2016) it was sought to generate 3D images of the soil to detect hydrocarbon contaminated water seepage. The Wenner arrangement was also employed successfully and contamination plumes have been identified (typically as resistivity dropped below 17 Ω·m).

In turn, Luz and Santana (1992) have studied (in pilot scale) the moisture evolution of iron ore sinter feed confined in a plywood container equipped with nine pairs of stainless steel electrodes (three rows of electrodes in three heights: bottom, middle and top).

In the classical electrical geophysical survey the Wenner α probe array (Wenner, 1915) should obey tree main principles in order to success: equal span between electrodes (***a*** = ***AM*** = ***MN*** = ***NB***), penetration depth of probes invariant and perfect collinearity of probes (perfect profile baseline). This kind of probe array was applied in this study aiming at to survey a wet quartz sand bed under dewatering on a pilot-scale vibrating screen. The screen dewatering operation was electrically monitored in different regions and depths of the wet granular bed.

As the screen used has effective area of 0.405 m², this would represent a small-scale experiment, because in typical field geophysical application the shortest distance between the poles (electrical probes) is usually 1 meter (***a*** ≥ 1 m), leading to arrays of at least 3 meters.

In order to verify the influence of small deviation of two of the basic statements for Wenner pattern on the moisture forecast, experiments were performed in a comparative basis. So the aim of this paper was to evaluate the effect of probe misalignment and variation in probe penetration depth on moisture determination by electrical resistivity method applied to a wet granular bed under dewatering.

## 2 MATERIAL AND METHODS

Firstly, a calibration curve was established to enable correlation between sand moisture and its electrical resistivity. In fact, electrolytic conductivity of interstitial water allows the application of this technique. 15 kg of quartz sand was homogenized in concrete mixer (volume of 0.120 m³) during 5 minutes with controlled moisture ranging from 5.0 % to 17.5 %. After homogenization the wet sand was poured into a hard plastic parallelepiped box, with the following dimensions: length of 0.500 m; 0.303 m width; and height of 0.158 m. A minimum of five measurements for each moisture condition were performed to determine the calibration curve. Three experimental campaigns have been carried out. Firstly “correct” or “standard” experiments — with the span regularity, collinearity, and constancy of penetration depth — were carried out. A second series of experiments was made, with intentional probe misalignment. The third test campaign was performed, once more with intentional departure from default Wenner’s parameters, in this case with variation in electrode penetration depths (spiking depth).

As shown by Pandey et al. (2015), using equipment very similar to one employed in the present work, the chemical composition of the electrodes has much less influence than the voltage and frequency of the electric current. Thus, copper electrodes were chosen, due to their easy availability.

For the implementation of each experimental campaign, each condition was tested employing two identical samples of quartz sand, with pre-established initial moisture (to allow bed dewatering tests in duplicate). Each sample was homogenized in a concrete mixer, for five minutes, then being placed on a pilot-scale dewatering screen (Figure 1). The standard condition (aligned array of copper probes or electrodes) and the abnormal array (with departure from the baseline) are shown in Figure 2 (vertical section) and Figure 3 (plant).

**Figure 1: Moisture profiling set up.**

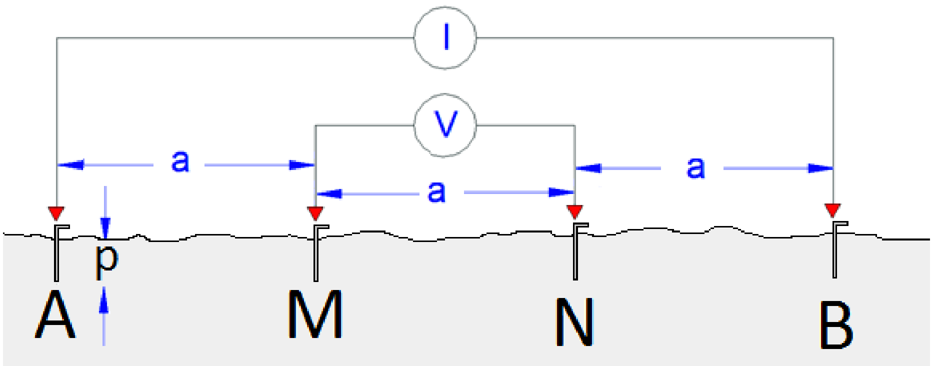


**Figure 2: Hypothetical bed vertical section and probe array for electrical profiling. Legend: A and B — current electrodes, M and N — potential electrodes; a — span (probe spacing); p — penetration depth of probes (spiking depth).**

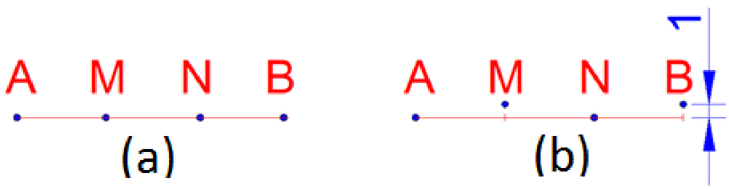


**Figure 3: Well aligned (a) and misaligned (b) profiling arrays (dimension in centimeter).**

After three minutes of bed vibration, electrical profiling was carried out with the resistivity meter (a microprocessor-based digital earth tester EM-4055), employing the Wenner array α, according to Equation (1). Plywood templates with holes corresponding to the correct and incorrect electrode array were applied, when appropriate (Figure 4). A minimum of five measurements for each of such dewatering experiment were performed.

$$\rho = \frac{4\pi R a}{1 + \frac{2a}{\sqrt{a^2 + 4p^2}} - \frac{a}{\sqrt{a^2 + p^2}}} \tag{1}$$

Where: ρ — apparent electrical resistivity (Ω·m); a — distance between probes (m); R — resistance value measured by the equipment (Ω); p — penetration depth of probes (m).

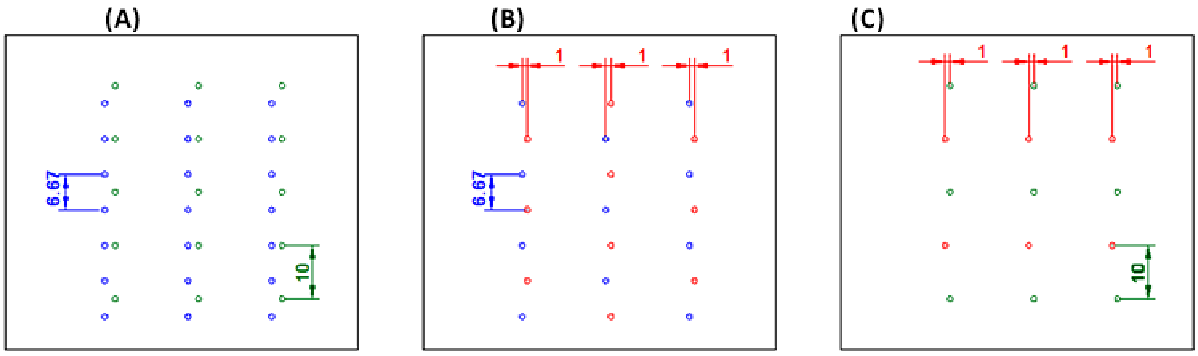


**Figure 4: Wooden templates for electrodes positioning (dimension figures in centimeters). (A): standard array (correct alignment template with two alternative probe spans: *a* = 6.67 cm and *a* = 10.0 cm); (B): misaligned array for span *a* = 6.67 cm; (C): misaligned array for span *a* = 10.0 cm.**

In turn, the penetration depth has been varied between 5.5 cm and 5.0 cm to evaluate the effect of this variation. It is appropriate to bear in mind that the standard depth of investigation of this method, as pointed out by Lasfargues (1957) and Pinto (2005), is 25 % of distance AB.

The average between the experiments and their duplicates (second bed), and the corresponding standard deviations were calculated, as well as the relative deviation between the experiments using the correct probe array and those ones using abnormal probe array. The moisture values of the profiling region were calculated employing the calibration curve. The electrical resistivity ratio was defined as:

$$d = \frac{\rho_w}{\rho_r} \tag{2}$$

HOLOS
ISSN 1807 - 1600

Where: d — electrical resistivity ratio; $\rho_w$ — apparent electrical resistivity from wrong probe array (Ω·m); $\rho_r$ — apparent electrical resistivity from right (standard) probe array (Ω·m).

The statistical variance of compound variable is a function of variances of its arguments (Spiridonov and Lopatkin, 1973; Wills and Napier-Munn, 2006). From Equation (1), the resistivity variance is given by Equation (3):

$$\sigma_\rho^2 = \left(\frac{\partial\rho}{\partial a}\right)^2 \cdot \sigma_a^2 + \left(\frac{\partial\rho}{\partial p}\right)^2 \cdot \sigma_p^2 + \left(\frac{\partial\rho}{\partial R}\right)^2 \cdot \sigma_R^2 \qquad (3)$$

Where $\boldsymbol{\sigma^2 i}$ stands for statistical population variance of parameter ***i***. Neglecting the variance of electrical resistance measurement, the errors theory can be treated according to the variance of the compound variable. Therefore, Equation (4) holds ($\Delta\imath$ stands for measurement error of ***i***).

$$\Delta_\rho^2 = \left(\frac{\partial\rho}{\partial a}\right)^2 \cdot \Delta_a^2 + \left(\frac{\partial\rho}{\partial p}\right)^2 \cdot \Delta_p^2 \qquad (4)$$

On line derivation tool by Wolfram Alpha (2016) gives these partial derivatives:

$$\frac{\partial\rho}{\partial a} = 4\pi Ra \frac{\left(\frac{a^2}{(a^2+p^2)^{\frac{3}{2}}} - \frac{2a^2}{(a^2+4p^2)^{\frac{3}{2}}} - \frac{1}{\sqrt{a^2+p^2}} + \frac{2}{\sqrt{a^2+4p^2}}\right)}{\left[1 + \frac{2a}{\sqrt{a^2+4p^2}} - \frac{a}{\sqrt{a^2+p^2}}\right]^2} \qquad (5)$$

And:

$$\frac{\partial\rho}{\partial p} = 4\pi R \frac{\left(\frac{ap}{(a^2+p^2)^{\frac{3}{2}}} - \frac{8ap}{(a^2+4p^2)^{\frac{3}{2}}}\right)}{\left[1 + \frac{2a}{\sqrt{a^2+4p^2}} - \frac{a}{\sqrt{a^2+p^2}}\right]^2} \qquad (6)$$

HOLOS ISSN 1807 - 1600

These latter expressions could be used to determine errors associated with variations in inter-electrode spacing and probe spiking depth. However, located variations have been adopted here (and further, destroying the collinearity). Thus, the approach via algebraic sensitivity analysis is not fully applicable to the processing of the results from the experimental campaigns herein.

## 3 RESULTS AND DISCUSSION

Quartz sand sample used has a size distribution well described by Hill distribution (with correlation $R^2 = 0.994$). This equation is given by:

$$Y = \frac{x^{4.390}}{x^{4.390} + \left(366.7\mu m\right)^{4.390}} \quad (7)$$

Where: ***x*** — particle size (µm); ***Y*** — mass fraction less than size ***x*** (-).

The obtained calibration curve is shown in Figure 5. As expected, the higher the interstitial moisture, the lower the granular bed resistivity. The calibration curve can be expressed analytically, after deletion of three outliers, by Equation (4). The regression's coefficient of determination obtained by *EasyPlot©* software for this equation was $R^2 = 0.9506$ and maximum deviation equal to 0.02728.

$$u = e^{\left[-0.001982(\rho+787.7)^{0.982}\right]} + 0.04970 \quad (8)$$

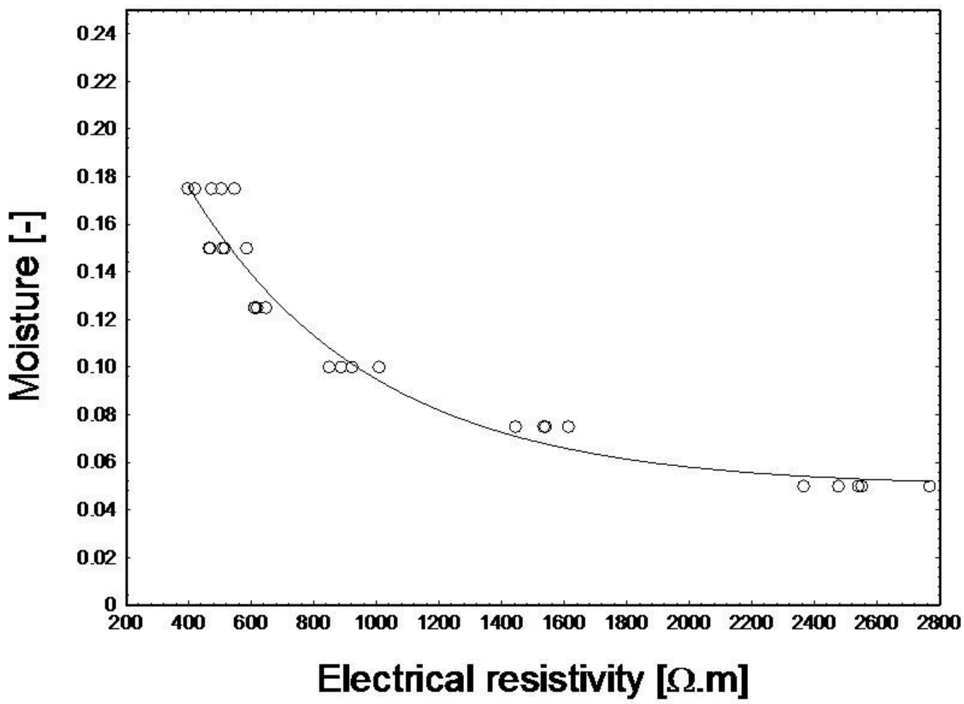


**Figure 5: Calibration curve of electroresistivity versus moisture (*u*).**

The average standard deviation of five readings for each moisture condition on the calibration curve was 63.63 Ω·m. This value was adopted as the maximum allowable for the standard deviation from experiment and its duplicate, obtained by electrical profiling (just for the case of correct Wenner $\alpha$ experiments). The results of these experiments conducted under the right Wenner's conditions are summarized in Table 1.

**Table 1: Experimental resistivity with correct probes pattern for selected spans, a, and penetration depth, *p*.**

| ***a*** **(m)** | ***p*** **(m)** | **Average (for two sand bed) (Ω·m)** | **Standard deviation (for two sand bed) (Ω·m)** |
|---|---|---|---|
| 0.0667 | 0.0550 | 918.36 | 5.15 |
| | | 891.20 | 5.15 |
| | | 781.25 | 0.47 |
| | | 788.53 | 7.03 |
| | | 961.58 | 4.45 |
| 0.1000 | 0.0550 | 917.38 | 13.91 |
| | | 759.56 | 41.13 |

HOLOS
ISSN 1807 - 1600

Adopting a hypothetical Gaussian variance equal to the discrepancy adopted with 95.45 % confidence level, the corresponding population standard deviation (square root of the variance) results equal to:

- For alignment: $\Delta a/2 = \sigma a = (0.100 - 0.0667)/2 = 0.0167$ m;
- For penetration depth: $\Delta p/2 = \sigma p = (0.050 - 0.055)/2 = 0.0025$ m.

Using these values (and the average resistance of 2063 ohm from tests) in Equations (4), (5) and (6), one would expect an average standard deviation 155.6 ohm.m for resistivity measurements, for this case. It is noteworthy that in the previous equations the variation in probe spacing does not take into account the loss of collinearity, as performed in present work.

The average standard deviation between experiments and their duplicates was 11.04 Ω·m, below the tolerance of 63.63 Ω.m. On the other hand, the results for the experiments under 1.0 cm misaligned electrode array (Figure 3-B) are shown in Table 2.

**Table 2: Experimental resistivity with misaligned electrical probes.**

| ***a*** **(m)** | ***p*** **(m)** | **Average (for two sand bed) (Ω·m)** | **Standard deviation (for two sand bed) (Ω·m)** | **Relative deviation from standard condition (%)** |
|---|---|---|---|---|
| 0.0667 | 0.0550 | 963.06 | 128.33 | 4.87 |
| | | 1031.95 | 26.23 | 15.79 |
| | | 1165.08 | 81.49 | 49.13 |
| | | 754.09 | 16.39 | -4.37 |
| | | 1022.26 | 63.11 | 6.31 |
| 0.1000 | 0.0550 | 1003.77 | 85.28 | 9.42 |
| | | 1061.08 | 0.60 | 39.70 |

As the experiments described in Table 2 did not meet (by adoption) the three conditions for correct application of Wenner's method, a standard deviation limit for evaluating these results was not considered. As a matter of fact, the aim was to observe what kind of errors could be generated. Thus, it can be concluded that probe misalignment leads to overestimated or underestimated results. On average, the expected relative deviation caused by this abnormal span was 17.26 % above the expected result.

The results from experiments with discrepancy on probe penetration depth, p, are shown in Table 3. Here, the electrodes with 5.5 cm depth were alternated with electrodes with 5.0 cm (as shown in Figure 6).

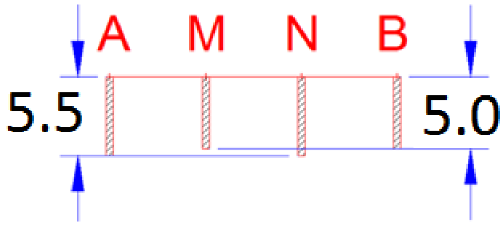


**Figure 6: Incorrect electrode penetration depths (dimension figures in centimeters).**

**Table 3: Experimental resistivity with discrepancy on penetration depth of electrical probes.**

| *a* (m) | *p* (m) | Average (for two sand bed) (Ω·m) | Standard deviation (for two sand bed) (Ω·m) | Relative deviation from standard condition (%) |
|---|---|---|---|---|
| 0.0667 | 0.0550 and 0.0500 | 1246.88 | 128.79 | 35.77 |
| | | 1299.54 | 91.80 | 45.82 |
| | | 1176.34 | 237.93 | 50.57 |
| | | 885.90 | 71.66 | 12.35 |
| | | 1332.32 | 132.54 | 38.56 |
| 0.1000 | 0.0550 and 0.0500 | 1404.08 | 64.72 | 53.05 |
| | | 1344.20 | 33.26 | 76.97 |

The differences in the penetration depth of the probes have caused overestimated resistivity values (Table 3). On average, the relative deviation was 44.73 % above the expected result (from standard experiments). The results, translated in terms of bed moisture, are summarized in Table 4.

**Table 4: Moisture values inside electrical profiling regions.**

| From standard experiments (%) | From misaligned probes (%) | From incorrectly penetrated probes (%) |
|---|---|---|
| 10.0 | 10.0 | 9.0 |
| 10.5 | 10.0 | 8.5 |
| 11.0 | 9.0 | 9.0 |
| 11.0 | 11.5 | 10.5 |
| 10.0 | 10.0 | 8.5 |

| | | |
|---|---|---|
| 10.0 | 10.0 | 8.0 |
| 11.5 | 9.5 | 8.5 |

One-factor analysis of variance was performed using data from Table 4, in order to detect significance of effects due misalignment and probe's depth spiking alteration. Only for convenience it was made normalization by dividing nominal values by the standard condition average (10.57 %). Tables 5 and 6 present ANOVA results for misalignment and discrepancy on penetration depth of probes, respectively.

**Table 5: ANOVA: standard system versus misaligned system.**

| *Variation source* | *Sum of squares (SQ)* | *Degreesof freedom* | *Mean Square (MQ)* | *Fisher's statistic F* | *P-value* | *Critical value of F* |
|---|---|---|---|---|---|---|
| Between groups | 0.01023 | 1 | 0.0102 | 2.40 | 0.14729 | 4.747 |
| Within groups | 0.05113 | 12 | 0.0043 | | | |
| Total | 0.06136 | 13 | | | | |

**Table 6: ANOVA: standard system versus depth-impaired system.**

| *Variation source* | *Sum of squares (SQ)* | *Degrees of freedom* | *Mean Square (MQ)* | *Fisher's statistic F* | *P-value* | *Critical value of F* |
|---|---|---|---|---|---|---|
| Between groups | 0.09204 | 1 | 0.0920 | 20.33 | 0.00072 | 4.747 |
| Within groups | 0.05433 | 12 | 0.0045 | | | |
| Total | 0.14637 | 13 | | | | |

In face of results from Table 5, the null hypothesis (the equality of the means of the two populations) cannot be rejected since the test statistic from the data is lesser than the F critical value (2.4 < 4.747). On the other hand, for values from Table 6, the decision is to reject the null hypothesis for because the test statistic from the data is greater than the F critical value (20.33 > 4.747). In effect, the very small value of p-value in Table 6 (p-value = 0.00072 < 0.001) is very strong evidence that the population means are really different.

The increase in penetration depth of the electrodes has led to the moisture underestimation in 100.00 % of experiments.

## 4 CONCLUSION

As seen from the analysis of variances carried out in this work, the electrode misalignment was not significant (within the conditions experienced). Contrary to this conclusion,

HOLOS ISSN 1807 - 1600

the discrepancy in the penetration of the electrodes proved to be highly significant, that is: differences in electrode penetration will induce errors in measuring the moisture content of the bulk material. As a matter of fact, the increase in penetration depth of the electrodes has led to the moisture underestimation in all experiments conducted to assess the impact of this penetration.

Anyway, attention should be paid to the three fundamental parameters of Wenner α electrical profiling. In laboratory scale, minimal disturbance can lead to ponderable errors, due to the small scale of the apparatus. Furthermore, conditions of granular medium confinement must be controlled for the specific application studied here. Variation in particle size distribution or porosity will lead to statistical noise, sometimes intolerable. The resistivity of interstitial fluid (water), of course, must also be monitored properly to enable the setting up of the corresponding forecast equation.

## 5 ACKNOWLEDGEMENTS

Taking the opportunity, the Authors acknowledge the following Brazilian institutions for their support: Brazilian Council for Technological and Scientific Development (CNPq), Foundation for Research Support of the State of Minas Gerais (FAPEMIG) and Brazilian Federal Agency for Support and Evaluation of Graduate Education (CAPES) for their financial support. The authors are also grateful to Mr. Celio Bibiano de Barros for providing polyurethane modular screen panels for the dewatering screen used and Dr. Maria Silvia C. Barbosa (Professor of Geophysics at Ouro Preto School of Mines) for helpful advice.

## 6 REFERENCES

Bristow, K. L. et al. (2001, May). A small multi-needle probe for measuring soil thermal properties, water content and electrical conductivity. *Computers and Electronics in Agriculture*, 31(3), 265–280. doi: 10.1016/S0168-1699(00)00186-1

Bui, Ph. T., Ogawa, Y., Nakarai, K., & Kawai, K. (2016, June) . Electrical resistance measurement to assess moisture transfer in cement-based mortar through water absorbing and drying processes. *Proceedings of The Japan Concrete Institute*, 38(1), 813–818.

Dahlin, T. & Loke, M. (1998, February). Resolution of 2D Wenner resistivity imaging as assessed by numerical modelling. *Journal of Applied Geophysics*, 38(4) 237–249. doi: 10.1016/S0926-9851(97)00030-X

Ding, J., & Chandra, R. (2018, October 7). Estimating soil moisture and electrical conductivity using Wi-Fi. *Microsoft Research.* https://www.microsoft.com/en-us/research/uploads/prod/2018/10/SMURF_TR-1.pdf .

Glover, P. W. J. (2010, April). The discovery of an anglo-saxon grubenhaus at new bewick, northern UK using electrical surveying and predictive deconvolution. *Archaeometry*, 52(2), 320–342. doi: 10.1111/j.1475-4754.2009.00468.x

Jolly (née moore), J. M., Beaven, R. P. and Barker, R. D. (2011, May). Resolution of electrical imaging of fluid movement in landfills. *Proceedings of the Institution of Civil Engineers - Waste and Resource Management,* 164(2), 79-96. doi: 10.1680/warm.2011.164.2.79

Lasfargues, P. (1957). *Prospection électrique par courants continus.* Masson & Cie.

Luz, J. A. M. & Santana, D. C. (1992). *Monitoramento de umidade em sinter feed por eletrorresistividade (Internal Report No. 1)*. Tecnomin — Projeto e Consultoria Ltda.

Morris, W., Moreno, E. I. & Sagüés, A. A. (1996, December). Practical evaluation of resistivity of concrete in test cylinders using a Wenner array probe. *Cement and Concrete Research*, 26(12), 1779–1787. doi: 10.1016/S0008-8846(96)00175-5

Neyamadpour, A., Wan Abdullah, W. A. T. & Taib, S. (2010, May). Use of four-electrode arrays in three-dimensional electrical resistivity imaging survey. *Studia Geophysica et Geodaetica*, 54(2), 299–311. doi: 10.1007/s11200-010-0016-8

Olayinka, A. I. & Yaramanci, U. (2000, September). Use of block inversion in the 2-D interpretation of apparent resistivity data and its comparison with smooth inversion. *Journal of Applied Geophysics*, 45(2) 63–81. doi: 10.1016/S0926-9851(00)00019-7

Pandey, L. M. S., Shukla, S. K., & Habibi, D. (2015, August). Electrical resistivity of sandy soil. *Géotechnique Letters* 5(3): 178-185. doi: 10.1680/jgele.15.00066

Pinto, E. (2005). *Melhoria e medição de terras: Medição da resistividade do solo: Método de Wenner.* Universidade do Porto.

Roodposhti, H. R., Hafizi, M. K., Kermani, M. R. S., & Nik, M. R. G. (2019, September). Electrical resistivity method for water content and compaction evaluation, a laboratory test on construction material. *Journal of Applied Geophysics,* 168, 49–58. doi: 10.1016/j.jappgeo.2019.05.015

Spiridonov, V. P. & Lopatkin, A. A. (1973). *Tratamiento matemático de datos físico-químicos*. Editorial Mir.

Thabit, J. M. & Khalid, F. H. (2015, December). Resistivity imaging survey to delineate subsurface seepage of hydrocarbon contaminated water at Karbala Governorate, Iraq. E*nvironmental Earth Sciences*, 75(1), 1–7. doi: 10.1007/s12665-015-4880-y

Valente, A. et al. (2006, November). Multi-functional probe for small-scale simultaneous measurements of soil thermal properties, water content, and electrical conductivity. *Sensors and Actuators A: Physical*, 132(1), 70–77. doi: 10.1016/j.sna.2006.05.010

Wenner, F. (1915, October). A method for measuring Earth resistivity. *Journal of the Washington Academy of Sciences*, 5(16), 561-563.

Wills, B. A. & Napier-Munn, T. (2006). *Mineral processing technology: An introduction to the* *practical aspects of ore treatment and mineral recovery.* Elsevier Sciente & Technology Books.

Wolfram Alpha. (2016, September 17). *Computational knowledge engine.* https://www.wolframalpha.com/input/?i=derivative.

## NOMENCLATURE

a — distance between probes (m);

d — electrical resistivity ratio (–);

p — penetration depth of probes (m);

R — resistance value measured by the equipment (Ω);

u — interstitial moisture of granular medium (–);

***x*** — particle size (μm);

***Y*** — mass fraction of particles less than size ***x*** (–).

Greek letters

$\Delta_i$— measurement error of parameter ***i*** (dimension of ***i***);

ρ — apparent electrical resistivity of granular medium (Ω·m);

$\rho_r$ — apparent electrical resistivity from correct (standard) probe array (Ω·m);

$\rho_w$ — apparent electrical resistivity from wrong probe array (Ω·m);

$\sigma^2_i$— statistical population variance of parameter ***i*** (dimension of ***i*** squared).

## COMO CITAR ESTE ARTIGO:

Reis, J. L., Da Luz, J. A. M., Vardanega, F. (2021). Perfilagem elétrica de desaguamento de areia induzido por vibração. *Holos*. 37 (7), 1-15.

## SOBRE OS AUTORES

**J. L. M. REIS**

Mestre em Engenharia Mineral (Área de Concentração: Tratamento de Minérios) pelo PPGEM UFOP, possui Bacharelado em Engenharia de Minas (2013) pela UNIPAC/FUPAC Lafaiete, com especialização técnica em metalurgia (2011) pela EPR Congonhas e formação técnica em mineração (2008) pela EPR Congonhas, além de conhecimentos avançados em informática

E-mail: jonathanleandro39@yahoo.com.br

ORCID ID: http://orcid.org/0000-0001-5390-5741

HOLOS
ISSN 1807 - 1600

**J. A. M. DA LUZ**
Departamento de Engenharia de Minas da Escola de Minas da UFOP; área de tratamento minérios.
E-mail: jaurelioluz@yahoo.com
ORCID ID: https://orcid.org/0000-0002-7952-2439

**F. VARDANEGA**
Graduado em Engenharia de Minas pela Universidade Federal de Ouro Preto (UFOP) em 2018. Consultor na área de engenharia de minas, em especial com emprego de recursos computacionais em planejamento de lavra de minas.
E-mail: fabio.vardanega@outlook.com
ORCID ID: http://orcid.org/0000-0002-5604-2395

**Editor(a) Responsável:** Francinaide Nascimento

**Pareceristas *Ad Hoc*:** LEANDRO PASA E EVANDRO KONOPATZKI